Extraction of Surface Topography from SAR Images Using Combined Interferometry and Stereogrammetry

Adrian Schubert, David Small, Erich Meier, Daniel Nüesch

Remote Sensing Laboratories, University of Zürich; Winterthurerstrasse 190; CH-8057 Zürich; Switzerland
Tel: +41 1 635 6523 FAX: +41 1 635 6842, Email: {schubert,daves,meier,nuesch}@geo.unizh.ch

Abstract

The high-resolution results obtained by interferometric SAR (InSAR) have been the main focus of research into digital surface model (DSM) generation in recent years. However, we demonstrate that initial processing of a SAR stereo pair for the same area can improve the InSAR result in three distinct ways: (a) by providing the input for synthetic phase generation and subsequent phase flattening, (b) by eliminating the need for manual selection of the ground control points (GCPs) required for phase calibration, and (c) by providing height estimates for missing InSAR-DSM values.
This technique was applied to data obtained by the European Space Agency's (ESA) ENVISAT and ERS-1/2 satellites for an area over Switzerland that includes rolling to mountainous terrain. ENVISAT provided the stereo acquisitions, ERS-1 and -2 the tandem interferometric dataset. It is shown that initial stereo processing makes InSAR DSM-estimation more reliable as well as fully automatable. Additionally, the stereo DSM is used to provide height estimates in areas where the InSAR processing failed.

1. Introduction

The motivation for pursuing the integration of stereo within an InSAR framework is to overcome the weaknesses of the latter method, namely:

- InSAR topography estimation requires a delicate **phase-unwrapping** step, which can be greatly aided by an existing low-frequency DSM.
- **GCPs are required** for interferometric phase calibration.
- Areas of low coherence in interferograms, due to temporal decorrelation in the multi-pass case, vegetation presence, and steep topography lead to **erroneous or missing height estimates**.

Although a stereo DSM will not provide nearly the height resolution of an InSAR DSM, InSAR processing can benefit from the availability of a stereo DSM in a number of ways, described in section 2.2.

2. Use of Stereo DSM during InSAR Processing

2.1 Stereo Processing

The stereo matching algorithm used during this work was first developed for optical stereo pairs by H-P. Pan in 1996 [2]. It was adapted for SAR stereo in 2001-2002 by Schubert et al. [3].

Besides the DSM, an important intermediate product stemming from the application of this algorithm to a stereo pair is the *match confidence* for all pixels within the stereo window. This is analogous to the coherence used in InSAR: the coherence can be used as an estimate of the quality of the measured differential phase, and similarly, the match confidence provides a quality estimate for the stereo heights derived from the estimated parallax field.

2.2 Stereo-Augmented InSAR Processing

The results from the stereo processor may be used at three points during the InSAR processing chain, each described briefly below.

2.2.1 Phase Flattening

Use of the coarse stereo DSM to calculate the expected phase, then subtracting this from the interferogram, reduces the number of fringe cycles dramatically. Subsequent phase unwrapping is therefore less error-prone than if an ellipsoid approximation is used for the topography.
The flattened phase is integrated over the scene in the next step. We employ the well-known branch-cut method first outlined by Goldstein et al. in [1]. While straightforward, this method tends to be extremely sensitive to phase noise, often resulting in large expanses of the interferogram that are marked as areas to avoid during the phase unwrapping.

2.2.2 Automatic Control Point Generation

Because the phase unwrapping solves for the relative phase only, a further phase calibration step is required before topographic heights can be calculated. This is typically done by selecting several control points in the SAR image for which heights and positions can be determined with the use of maps. A more elaborate method involves the placement and positional measurement of reflectors in the terrain prior to the data acquisition.
The stereo DSM, which is produced without the use of GCPs, is a clear potential source of height control points that can be used for phase calibration. Indeed, as many points as there are pixels are available, but naturally their quality is unknown. We apply three constraints to the stereo DSM in order to aid the automatic point selection:

- The match confidence must be greater than an empirically-determined threshold.
- The SAR pixel brightness must be greater than a given

threshold, so that height values obtained for water and radar shadow will not be considered.

- The interferometric phase must have a local standard deviation below a given threshold, as local averaging is done during phase calibration.

By applying these criteria to the stereo DSM, a high number of candidate points usually remain. Final point selection is performed by placing a square grid over the DSM and extracting the candidates at the grid intersections. This ensures a regular distribution of control points over the whole scene.

2.2.3 Hole-Filling

If significant holes remain in the final InSAR DSM, it is possible to obtain some height information for these regions from the stereo DSM. By applying the match confidence and brightness criteria used during automatic GCP selection, we can augment the InSAR holes with stereo heights meeting our requirements. This results in holes with a rather speckled appearance, since only stereo heights of sufficient quality were selected.

A last step is taken in order to give the DSM a smoother appearance, while leaving remaining larger holes untouched; it is clearly undesirable to interpolate the data across large expanses. The problem is solved here using a two-step technique:

- A binary holes-mask is calculated for the DSM, and is subjected to a morphological *closure* operation [4]. This eliminates holes of a size below a given threshold, while leaving the larger holes intact.
- A cubic interpolation over a Delaunay triangular network is then performed for all missing data except those within large holes, as given by the binary mask from the first step.

3. Experimental Datasets

A pre-condition to performing stereo-aided InSAR is the existence of a stereo pair whose overlap region (stereo window) coincides at least in part with that of the interferometric acquisition. This experiment used a stereo tandem pair from ESA's spaceborne platform for earth observation ENVISAT, and an interferometric tandem pair from ERS-1/-2, also from ESA, over a region covering a part of Switzerland including Zurich. The heights span a range of about 2000 m across the stereo-InSAR overlap region.

The ENVISAT C-band data used were slant-range complex images obtained in image mode from descending orbits six days apart, in September 2003. A stereo intersection angle at scene center of about 12° was available from beams 3 and 6.

The interferometric ERS-1/2 tandem acquisition is from descending orbits, taken one day apart in October 1995, also in C-band.

The stereo window resulting from the ENVISAT pair covers approximately 60% of the ERS scenes; it is only within this region that stereo-augmented InSAR is possible.

4. Results and Discussion

4.1 Phase flattening

The stereo DSM obtained using the ENVISAT pair is shown in Fig. 1. The effect of using it for phase flattening of the interferometric pair is shown in Fig. 2 for a ~28 x 28 km area south of the Zurich Lake. If an ellipsoid model is used to generate the synthetic phase, and this is then subtracted from the measured phase, the result still displays a

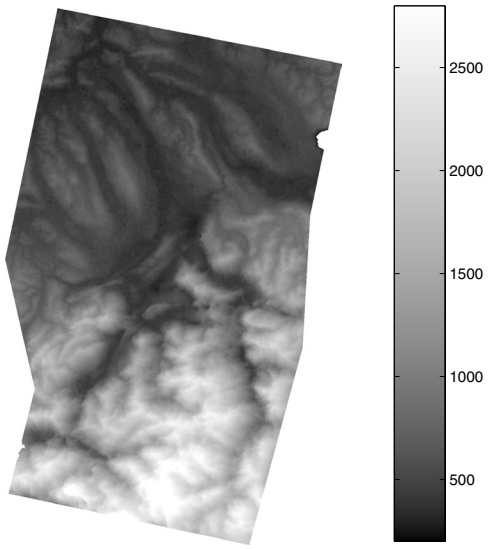

Fig. 1. ENVISAT stereo DSM for the Zurich site [m]

(a)

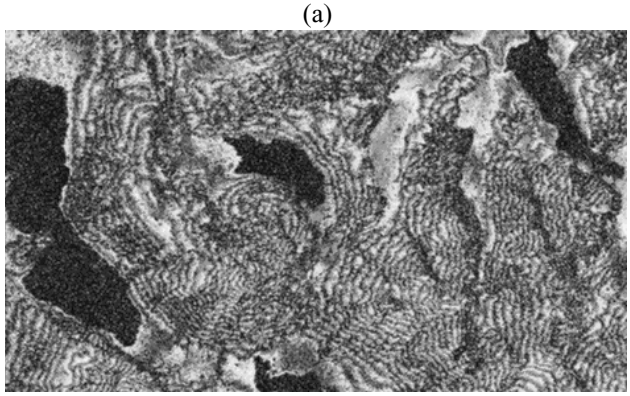

(b)

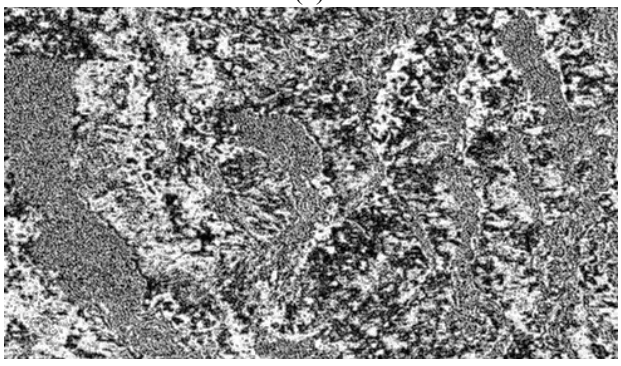

Fig. 2. Flattened phase using (a) ellipsoid terrain model (b) stereo DSM

high fringe density (Fig. 2a). If, however, the existing low-frequency stereo DSM is used for the synthetic-fringe generation, the result is a residual phase field without obvious fringe cycles (Fig. 2b). This situation makes accurate integration of the phase over the entire scene a simpler task, thus improving the final DSM accuracy.

The DSM resulting from InSAR processing with the stereo-based phase flattening just described is shown in Fig. 3. Many holes still remain in spite of the flattening, due to low coherence mainly over water bodies, in steep terrain, and areas of lower signal return, all creating phase noise too great for the branch-cut algorithm to deal with. Nevertheless, the quality of the data that is processed to the end is quite high, which can be confirmed by subtracting it from a reference digital elevation model (DEM); this is done for the final product, as seen later in Fig. 6.

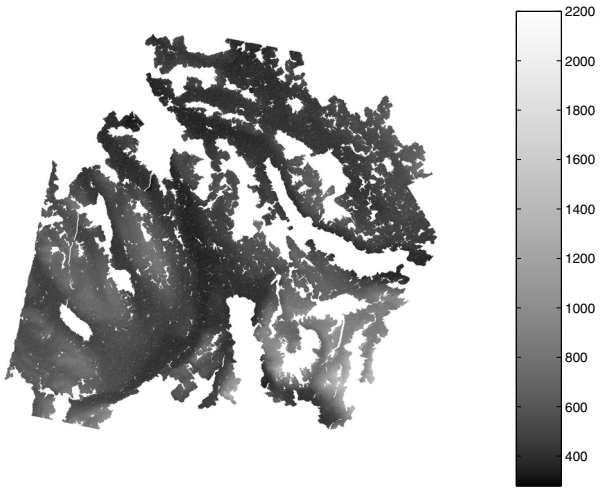

Fig. 3. InSAR DSM obtained using stereo DSM during phase flattening [m]

4.2 Automatic Control Point Generation

If the GCPs to be used for phase calibration are chosen at random from the stereo DSM, it is expected that the error statistics will reflect those of the entire DSM. It follows that if we perform a statistical validation of our automatically-selected, constrained set of points, the resulting error statistics should reflect those of an improved DSM. In particular, the standard deviation should be much lower for a selected set of high-quality points.

This is indeed the case for our automatically-generated points. We compared both the GCP list and the original stereo DSM to a high-quality height model with 25 m grid spacing. The 44-point GCP list has a mean error of 2.6 m with a standard deviation of 19.8 m. In comparison, the entire stereo DSM has a mean error of -13.8 m and a standard deviation of 112.0 m.

Clearly the GCP selection criteria succeed in greatly increasing the reliability of the points. In addition, the high number of points and their regular distribution make the phase calibration consistent across the scene, as can be judged by the final results.

4.3 InSAR Hole Augmentation

The result of the hole augmentation described in section 2.2.3 can be seen in Fig. 4. The speckled appearance is due to the addition of stereo heights chosen according to the criteria described in sections 2.2.2 and 2.2.3. Large holes such as water bodies and areas that could not be unwrapped, and for which no good stereo heights were available, are left untouched.

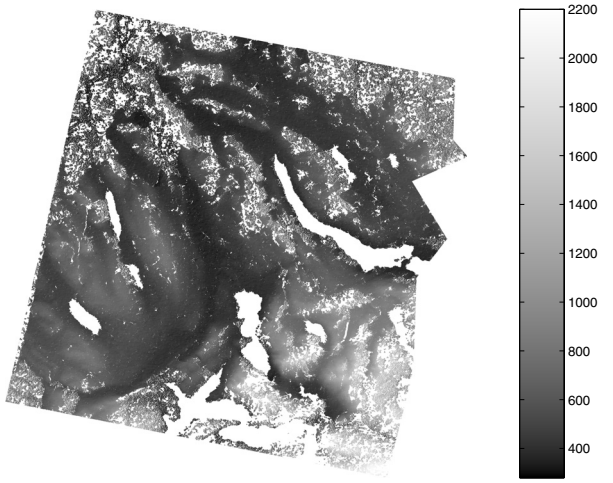

Fig. 4. InSAR DSM after augmenting the holes with selected stereo-DSM heights [m]

4.4 Data Closure and Interpolation

The strong visual effect of the cubic interpolation combined with the morphological closure is clearly visible in Fig. 5. Most of the remaining holes are due to water bodies, which is expected. Some smaller remaining holes are scattered throughout the image; these are due to holes that had sizes just above the “large-hole” threshold, and were therefore not interpolated across.

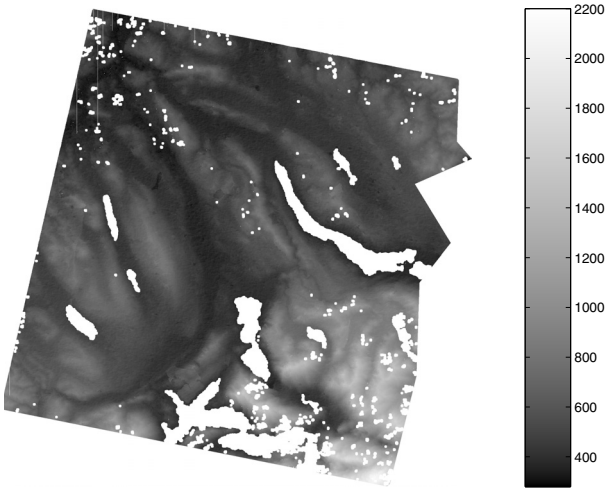

Fig. 5. InSAR DSM after closure and cubic interpolation to fill in the smaller holes [m]

4.5 Comparison to the Reference DEM

The effectiveness of the stereo-aided method as compared to unaided InSAR is clear by comparing the errors in the final DSMs obtained by each method.

Fig. 6 is the difference between the stereo-aided DSM and the reference DEM. Several phase-unwrapping errors are

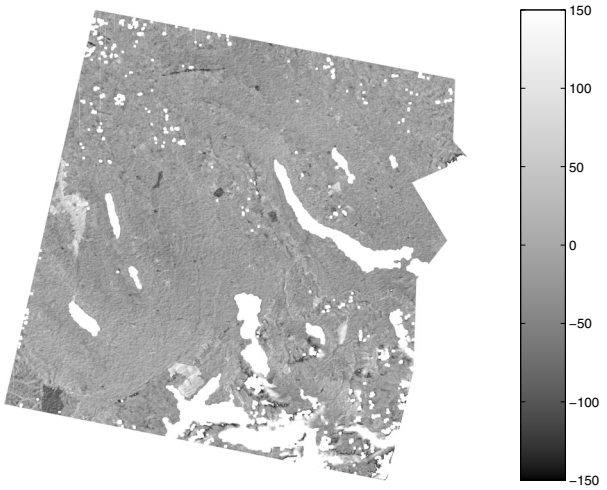

Fig. 6. Difference between the final stereo-aided InSAR DSM and the reference DEM

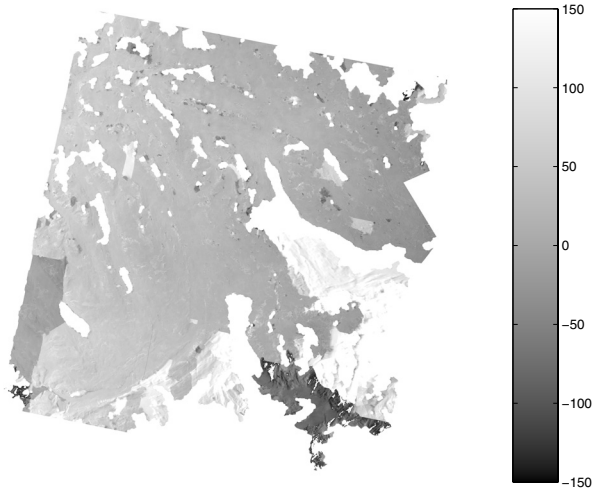

Fig. 7. Difference between the final unaided InSAR DSM and the reference DEM

visible as dark and light regions, for example on the left-central and lower-left DSM edges. These areas indicate failed phase integration. In the lower-right of the DSM, some areas of overestimation in the valleys between the mountain ranges are visible. These are examples of failed stereo-DSM augmentation. Although the selection criteria are sufficient in flat to rolling terrain, performing stereo in the mountains clearly presses the method to its limits.

In stark contrast to the stereo-aided result, Fig. 7 shows the errors resulting from the unaided processing chain. Many regions have been incorrectly unwrapped, and even the flatter terrain has been consistently overestimated.

The statistical description of these errors are given in Table 1. With nearly 86% of its points under 40 m absolute height error, the stereo-aided DSM is far superior to the unaided one, having only 54% of its pixels under 40 m. We stress that it is not absolute DSM accuracy that is the goal of this technique. Rather, it is that the use of parallel **stereo processing can greatly improve the *achievable* InSAR result**, while making the processor automatable at the same time.

TABLE 1: ERROR STATISTICS FOR STEREO-AIDED AND UNAIDED INSAR DSMS

Experiment	Stereo-aided DSM	Unaided DSM
Mean error [m]	-10.8	36.4
Std dev [m]	35.8	60.1
Pixels with < 20 m error [%]	54.6	27.3
Pixels with < 40 m error [%]	85.6	54.0
Pixels with < 100 m error [%]	98.3	88.5
Pixels with < 200 m error [%]	99.5	98.1

5. Conclusions and Outlook

By using a low-resolution DSM obtained by stereo matching, it is possible to greatly improve the quality and the coverage of an InSAR DSM generated for the same area. This is not achieved merely through a classical fusion of the two end-products. Rather, it is the combination of the stereo match confidence and the actual height values that yield the maximum benefit. The technique is especially useful when no reliable lower-frequency height model is already available.

Future versions of this combined technique will include an updated phase-unwrapping algorithm based on statistical cost-flow optimization. The technique is currently also being tested on airborne datasets, where a much better height resolution can be achieved over smaller areas than for spaceborne sensors.

6. Literature

[1] Goldstein, R.A., Zebker, H.A., and Werner, C.L., *Satellite Radar Interferometry: Two-Dimensional Phase Unwrapping*, Radar Science, Vol. 23, No. 4, pp. 713-720, 1988.

[2] Pan, H-P.: *General stereo image matching using symmetric complex wavelets*. Wavelet applications in signal and image processing IV, Proc. SPIE 2825, pp. 697-721, 1996.

[3] Schubert, A., Small, D., Meier, E., and Nüesch, D., *Robustness of Wavelet-Based Stereo Matching for Variable Acquisition Geometries Using Simulated SAR Images*, Proc. IGARSS'02, Vol. 5, pp. 2759-2761, 2002.

[4] Serra, J., *Image Analysis and Mathematical Morphology*, Academic Press, U.S.A., 1982.